Effect of Filler Distribution on Fracture Resistance of Modern Dental Composites

by

Carolina Wentworth

Thesis submitted to the Faculty of the
Advanced Education in General Dentistry (2yr) Graduate Program as supported by
Uniformed Services University of the Health Sciences
In partial fulfillment of the requirements for the degree of
Master of Oral Biology 2019

Distribution Statement

Distribution A: Public Release.

The views presented here are those of the author and are not to be construed as official or reflecting the views of the Uniformed Services University of the Health Sciences, the Department of Defense or the U.S. Government.

UNIFORMED SERVICES UNIVERSITY OF THE HEALTH SCIENCES
POSTGRADUATE DENTAL COLLEGE
SOUTHERN REGION OFFICE
2787 WINFIELD SCOTT ROAD, SUITE 220
JBSA FORT SAM HOUSTON, TEXAS 78234-7510
https://www.usuhs.edu/pdc

THESIS APPROVAL PAGE FOR MASTER OF SCIENCE IN ORAL BIOLOGY

Title of Thesis: "Effect of Filler Distribution on Fracture Resistance of Modern Dental Composites"

Name of Candidate: Carolina Wentworth
Master of Science Degree
May 21, 2019

THESIS/MANUSCRIPT APPROVED: DATE:

[redacted]

William J. Greenwood, COL, DC
DEAN, FORT HOOD AEGD 2-YR RESIDENCY
Committee Chairperson

05/21/2019

[redacted]

Michael Mansell, LTC, DC
DIRECTOR FORT HOOD AEGD 2-YR RESIDENCY
Committee Chairperson

05/21/2019

[redacted]

John D. King
ASSISTANT DIRECTOR FORT HOOD AEGD 2-YR RESIDENCY
Committee Member

05/21/2019

The author hereby certifies that the use of any copyrighted material in the thesis/ dissertation manuscript entitled:

"Effect of Filler Distribution on Fracture Resistance of Modern Dental Composites"

is appropriately acknowledged and, beyond brief excerpts, is with the permission of the copyright owner.

Carolina Wentworth
Fort Hood AEGD 2-YR Residency
Uniformed Services University
05/21/2019

ACKNOWLEDGMENTS

I would like to acknowledge Lt Col Wen Lien for dedicating his time and providing guidance during this joint project with the United States Airforce. I would also like to acknowledge the support of the Dental Evaluation and Consulting Services (DECS) for allowing the use of testing equipment to take this project to fruition.

Furthermore, I would also like to thank LTC Michael Mansell and MAJ John King and the United States Army for mentorship and support during each step of this project.

DEDICATION

I would like to dedicate this project to my husband and son, without your effort and support I would not have been able to accomplish this great achievement of becoming a Comprehensive Dentist and continue my career as a soldier.

COPYRIGHT STATEMENT

DISCLAIMER

The views presented here are those of the author and are not to be construed as official or reflecting the views of the Uniformed Services University of the Health Sciences, the Department of Defense or the U.S. Government.

ABSTRACT

Effect of Filler Distribution on Fracture Resistance of Modern Dental Composites

Carolina Wentworth, DDS, 2019

Thesis directed by: Lt Col Wen Lien, USAF Dental Evaluation & Consultation Service (DECS), San Antonio, TX; LTC Michael R. Mansell, United States Army Advanced Education in General Dentistry Fort Hood, TX.

Introduction: Failure of dental composite restorations is closely associated with the fracture processes of the filler-matrix systems.
Objective: The purpose of this study is to investigate how various filler-matrix systems (i.e., hybrid, nanohybrid, and microfill) with different microstructural characteristics and filler distributions (i.e., unimodal, bimodal, and multimodal) can influence time-dependent fracture resistance of resin based composites.
Materials and Methods: Twenty rectangular (2.75x5x25mm3), single-edge notch specimens (2.5mm notch depth) per composite (n=20) were made from a stainless steel mold with a razor blade insert. The samples were tested using a universal testing machine (Instron ElectroPuls E3000). Fracture toughness, K_{IC} [MPa m0.5], values were calculated via measurements from the 3-point bending test (span = 20 mm, cross-head speed = 0.5 mm/min) applied on the single-edge notched-bend specimens. Composite microstructural features were analyzed by scanning electron microscopy and laser diffraction particle size analyzer. Filler content was measured by thermogravimetric analysis. All specimens were stored in 37°C distilled water for 24 hours prior to testing. Data were analyzed with ANOVA/Tukey (α=0.01) and regression.
Results: Fracture toughness values were found – rankings in descending order were: Nanohybrids > Hybrids > Microfills. Additionally, composites with multimodal distribution demonstrated significantly less fracture resistance than composites with either unimodal or bimodal distribution.
Conclusion: Fracture toughness as a function of filler content increased with percent filler weight. In a similar behavior, fracture toughness as a function of filler size range exhibited the highest fracture resistance at 750nm. However, composites containing nano-fillers showed significantly higher fracture resistance than composites containing only micro-fillers.

TABLE OF CONTENTS

LIST OF TABLES

LIST OF FIGURES

Effect of Filler Distribution on Fracture Resistance of Modern Dental Composites

Introduction

Multifaceted research in dental materials has a very important role in the application of scientific evidence into clinical practice. Past studies have attempted to understand degradation, fatigue, and failure of resin based composites (RBC). Recently, there has been a renewal of interest in the understanding of filler technology and its implications in physical properties and clinical performance of RBCs. This renewed interest leads us to ask the following questions: (1) Does different filler composition, size, and morphology affect the physical properties of modern RBCs, and (2) does fracture toughness vary across different classes of RBC (i.e., nanofill, microfill, and nanohybrid)?

RBC Classification

Dental RBCs have evolved significantly since their first introduction more than 50 years ago (Ferracane, 2012). RBCs, scientifically referred to as particulate-reinforced polymer matrix composites, are a heterogeneous mixture. This mixture consists of resin (organic polymer matrix), fillers (inorganic particles), coupling agents (silane), and the initiator-accelerator system (initiators: iodonium salts, benzoyl peroxide; accelerators: organic amines like camphoroquinone) (Sakaguchi & Powers, 2012).

The uncured organic matrix consists of various monomers and oligomers such as bisphenol A-glycidyl methacrylate (BISGMA), urethane dimethacrylate (UDMA), or triethylene glycol dymethacrylate (TEGMA). The inorganic filler, is commonly made of finely ground quartz or glass, sol-gel derived ceramics, microfine silica, or more recently

nano-silica particles. Fillers, made of colloidal silica particles, have low coefficients of thermal expansion and a diameter less than 0.1 micron, and have improved condensability and polishability (Farah & Powers, 1991). Polishability of a resin composite is affected by the filler particle size. The smaller the particle the higher the polish and polish durability. These can be seemed in nanofilled composites. The addition of nanoparticles improves the polishability and retention of the initial gloss, nanoclusters shear at a rate similar to the surrounding matrix abrasion. This allows for long term polish retention (Sakaguchi & Powers, 2012).

Silane coupling agents, mainly 3-methacryloxypropyltrimethoxysilane (MPS), improve the RBC's physical properties by preventing hydrolytic breakdown along the filler-matrix interface. This inhibits cracking of the resin by allowing stress transfer between the filler and matrix. Organosilanes, the most common coupling agents, serve as bifunctional molecules. On one end the silane group bonds to the hydroxyl groups on the filler particles via a condensation reaction that produces a siloxane bond. The methacrylate group on the other end undergoes addition polymerization with the resin based composite during light- or chemical-activation of the resin matrix (Tyas et al, 1988).

RBCs have multiple modes of cure: chemical, light activated, or both. For chemically-activated resin composites, benzoyl peroxide and tertiary amines serve as the source of free radicals (tertiary amines such as N,N-dihydroxyethyl-p-toluidine). On the other hand, light-activated resin composites use a diketone photoactivator, such as camphoroquinone, in conjunction with a tertiary aliphatic amine, such as 4-N,Ndimethylaminophenythyl alcohol (Nadarajah, Neiders, Cohen, 1997).

Mechanical Properties

Randolph et al; concluded that RBC filler characteristics (such as composition, size, and morphology) can influence their physico-mechanical properties. The RBCs tested showed variability regarding filler shape, content, and distribution (nanohybrids, nanoparticles (<100 nm) and sub-micron particles (≤1μm)). The research focused on flexural modulus, flexural strength, and micro-hardness. Flexure was tested after aqueous incubation of the sample using a universal testing machine with a 3 point bending jig. Surface hardness was tested by using a Vickers indenter to determine the ability of the sample to resist plastic deformation. Their data showed that the resin composite with the highest physico-mechanical properties also had the highest filler contents and exhibited the lowest solvent sorption. From their findings it can be deduced that filler content plays an important role in RBCs physical and mechanical properties.

Fracture resistance plays a vital role in resin based composite. Fracture toughness (K_{IC}) is a measure of a material's resistance to the propagation of a crack from a preexisting flaw of known size and infinite sharpness, i.e. a pre-crack. K_{IC} is an inherent property of a material, and therefore its value should be independent of testing modality or specimen geometry (Illie et al, 2017).

Thomaidis et al, concluded that fracture toughness varies within the different classes of RBCs. The research focus on the following mechanical properties: 1)Flexural Modulus and Flexural Strength (three point bending), 2)Brinell Hardness, 3)Impact Strength, mode I and mode II; 4)Fracture toughness employing SENB and Brazilian tests, and 5)Fractography. In this study, different classes of RBCs showed difference in fracture toughness as filler volume decreased; microhybrids had increased fracture toughness

values when compared to other categories (microhybrids > nanofills > ormocer > nanohybrids).

Significance

Modern dental restorative composites exhibit features on more than one length scale, ranging from nano- and micro-fillers, to the polymerized macro-state of a high-molecular-weight polymeric matrix. (Randolph, Palin, Leloup, Leprince, 2016). This heterogeneous system can play a vital role in determining the bulk material properties and is likely to contain defects or flaws, ranging from millimeters down to nanometers or atomic scale, which can give rise to viscoelastic behavior, manifested as elastic bending or torsion. However, if stresses applied to this "composite solid" are too excessive, these structural flaws can become unstable and propagate catastrophically, culminating in bulk fracture. Thus, failure of dental composite restorations is closely associated with the fracture processes of the filler-matrix systems (Ilie, Hickel, Valceanu, Huth, 2011). It is the interest of this study to explore the relationship between structural defects and fracture resistance and to understand the effect of a heterogeneous system like dental composite, which contains at least two hierarchy levels, on fracture mechanics. The null hypothesis is: There exists no causal relationship between the dependent variable, fracture toughness, and the included independent variables matrix chemistries, filler morphologies, distributions, and size for various modern filler-matrix systems such as hybrid, microfill, and nanohybrid composites.

Materials and Methods

K_{IC} Fracture Toughness

Fracture toughness was measured by a single-edge notched beam method [ASTM E399-83]. To prepare each specimen, a knife-edged split (2 mm x 2 mm x 25 mm) aluminum mold (Sabri, Downers Grove, IL, USA), was lightly lubricated with a nonreactive lubricant (Vaseline Petroleum Jelly) and then placed on a Mylar strip-covered glass slide. Twenty specimens per each of RBC (n = 20, *Table 1*) were made by inserting the restorative material into the mold until completely filled. The top surface of the mold was then covered with a second Mylar strip and glass slide to ensure that the end of the specimen is flat with parallel surfaces. One end of the specimen was then exposed to a light-curing-unit (ParadigmTM, 3M, St. Paul, MN, USA) for 20 seconds each in overlapping increments. Next, the mold was turned over, and the opposite side of the specimen were exposed to the light in a similar manner. The specimens were then stored in 37 °C distilled water for 24 hours. At 24 hours, the notched specimens were fractured in a Universal Testing Machine (ElectroPuls E3000, Instron, Canton, MA, USA) at a cross-head speed = 0.5 mm/min. For the purposes of testing, the notch on each specimen was oriented to the tensile side and the loading pin aligned with the notch.

The load-deflection curves were recorded. Height, *h*, (mm), and width, *w* (mm), of the specimens were measured with an electronic digital caliper (GA182, Grobet Vigor, Carlstadt, NJ). The notch depth was measured, *a* (mm), with a stereo microscope (Nikon Measure-scope MM-22, Nikon, Tokyo, Japan) and a digital measuring and recording device (Quadra-Chek® 200, Metronics Inc., Bedford, NH, USA) at 10X magnification.

Fracture toughness (KIC, MPa m0.5) was calculated from measurements with the single-edge notched-bend specimens using the formula:

$$K_{IC} = 3\left(\frac{a}{w}\right)^{1/2}\left\{\frac{1.99-\frac{a}{w}\left(1-\frac{a}{w}\right)\left[2.15-3.93\left(\frac{a}{w}\right)+2.7\left(\frac{a}{w}\right)^{2}\right]}{2\left(1+2\frac{a}{w}\right)\left(1-\frac{a}{w}\right)^{3/2}}\right\}\left(\frac{P\,S}{h\,w^{3/2}}\right)$$

where *P* (N) is the load and S (mm) is the 20 mm span distance between supports.

Thermogravimetric analysis (TGA)

TGA measurements were performed using a TGA/DSC 1 instrument (Mettler Toledo, Columbus, OH, USA) connected to a mass spectrometer (ThermoStar, Pfeiffer Vacuum, Asslar, Germany). Each RBC sample, 30-60 mg per composite, were weighed on an analytical balance (XS105 Dual Range, Mettler Toledo, Columbus, OH, USA) and placed in a 70 µl alumina crucible. After the sample insertion, the sample chamber was purged with nitrogen (10 mL/min) and heated in order to eliminate all components present, except the filler. Temperatures were ramped from room temperature to a final temperature of 900 °C at a heating rate of 10 °C/min. The filler content of each RBC sample was determined from the TGA curve using proprietary software (STARe, Mettler Toledo, Columbus, OH, USA).

Structural Characteristics

Composite microstructural features were examined by scanning electron microscopy and a laser diffraction particle size analyzer. Filler sizes and distributions were assessed by weighing a sample of ~ 0.3 g ± 0.05 g per RBC brand. The samples were dispersed in 20ml aliquot of acetone and ethanol and agitated to maximize particle de-agglomeration. The samples were transferred into a cuvette and filler sizes were

assessed via a dynamic light scattering approach (Zetasizer Nano ZS). Light scattering method analyses the Brownian motion of particles in a liquid suspension. Filler and matrix microstructural features were analyzed by scanning electron microscopy (irregular vs spherical).

Statistics

Data were analyzed with ANOVA/Tukey (α=0.01) and regression.

Table 1. *Resin base composites and specifications.* *(manufacturer data)*

Composite	Manufacturer	Material Class	Filler Weight (%)	Filler Volume %	Filler Content (size of content)	Type of matrix	Depth of Cure	Curing Time	Curing Wavelength
Activa BioActive	Pulpdent	RMGIC-like	56%	-	-	Ionic resin maxtrix	4 mm	20 sec	-
Admira Fusion	Voco	Nano-hybrid	84%	-	Nano, glass ceramic	Ormocer-(SiO2 backbone), no traditional monomers	2.7 mm	20 sec	-
Beautifil Bulk	Shofu	High Viscosity Giomer (Hybrid)	87.00%	74.50%	S-PRG filler based on fluoroboroaluminosilicate	Bis-GMA, UDMA, Bis-MPEPP,TEGDMA	4mm	10 sec	-
Beautifil Bulk Flow	Shofu	Low Viscosity Giomer (Hybrid)	72.50%	51%	S-PRG filler based on fluoroboroaluminosilicate	Bis-GMA, UDMA, Bis-MPEPP,TEGDMA	4 mm	10 sec	-
Beautifil II	Shofu	Hybrid/ Giomer	83.30%	69%	0.01um-4.0 um	Bis-GMA, TEGDMA	5.9 mm	20 sec	-
Durafill VS	Kulzer	Microfill	-	66%	Silicon dioxide, 0.02-0.07 um, splinter polymer < 20 um	Bis-GMA, TEDGMA, urethane dimethacrylate	2 mm	20-40 sec	460-470 nm
Epic-TMPT	Parkell	Microfill	-	-	Proprietary	TMPT (proprietary)	-	20-40 sec	-
Filtek One Bulk Fill	3M	Bulk Fill nano-hybrid	76.50%	58.50%	20nm Silica, 4-11nm Zirconia, Ytterbium trifluoride 100 nm	AUDMA, AFM, DDDMA, UDMA	5mm	10-20 sec O/B/L	-
Filtek Supreme Ultra	3M	Nano-hybrid	78.50%	63.30%	20 nm silica, 4-11 nm zirconia, aggregated zirconia/silica nanoclusters	Bis-GMA, UDMA, TEGDMA, Bis-EMA(6)	2 mm	20 sec	400-500 nm
Kalore	GC America	Nano-hybrid	82%	-	400 nm modified strontium glass, 100nm lanthanoid fluoride,16nm dispersed silica (17 um PPFs)	UDMA, dimethacrylate co-monomers, DX-511	2.5mm	20 sec	-
Majesty Posterior	Clearfil	Nano-hybrid	92%	82%	1.5um glass filler, 20nm alumina microfiller	Bis-GMA, TEGDMA, hydrophobic aromatic dimethacrylate	1.5 mm	20 sec	400-515nm
N'Durance	Septodont	Nano-hybrid	80%	65%	40 nm ytterbium fluoride, silanated 500 nm barium glass and 10 nm silica	ethoxylated BisGMA, UDMA and the new dicarbamate dimethacrylate dimer acid	2.5 mm	30 sec	470-480 nm
Point 4	Kerr	Microhybrid	76%	57%	0.4 um	Bis-GMA	2 mm	40 sec	-
Renamel	Cosmedent	Microfill	70%	60%	.04-2um pyrogenic silica acid	Bis-GMA, Bis-EMA	2mm	20-40 sec	400-500nm
Renamel Nano Plus	Cosmedent	Nano-hybrid	78%	60%	0.02-0.7um silica, Ba-Al-Fluro borosilica	BDDMA, Bis-GMA, UDMA	2 mm	20-40 sec	400-500 nm
SonicFill 2	Kerr	Bulk Fill Nano-hybrid	81.35%	-	Silica, Barium glass, YbF3, mixed oxides	Dimethacrylates, Bis-GMA, Bis-EMA	5mm	20sec	400-520 nm
Tetric Evo Ceram	Ivoclar Vivadent	Nano-hybrid	76.00%	55%	40nm-3um Ba glass, ytterbium trifluoride, mixed oxides	Bis-GMA, Urethane dimethacrylate, Ethoxylated Bis-EMA	2mm	10 sec	400-500nm
TPH Spectra HV	Dentsply-Sirona	Nano-hybrid	77.20%	57.00%	Silanated Ba-Br-F-Al silicate and silicon dioxide 1.35 um	urethane modified Bis-GMA, TEGDMA, polymerizable dimethacrylate resin	2 mm	10 sec	470 nm
Venus Diamond	Kulzer	Nano-hybrid	81%	64%	5nm-20um, Barium aluminum fluoride glass, discreet nanoparticles	TCD-DI-HEA, UDMA	2 mm	20-40 sec	440-480 nm
Venus Diamond Flow	Kulzer	Nano-hybrid	65%	41%	0.02 um-5 um Ba-Al-F silicate, YbF3, SiO2	UDMA, EBADMA	2 mm	20 sec	440-480nm

Results

Variations in the fracture toughness were noted between the different groups of materials tested. Fracture toughness values were found – rankings in descending order were: Nanohybrids > Hybrids > Microfills (Table 2).

Additionally, composites with multimodal distribution demonstrated significantly less fracture resistance than composites with either unimodal or bimodal distribution (Figure 1& 3). The fracture toughness of composite systems adopted with new polymeric matrix chemistries (i.e., ormocer, dimer acid-base, giomer, and DX-511 monomers) were not statistically different than methacrylate-based systems (Fig 1).

Moreover, fracture toughness (K_{IC}) as function of the independent variable (filler weight %) showed an increased in fracture toughness (K_{IC}) as filler weight increases until a critical value of 75%. After this value a decreased in fracture toughness was observed.

Table 2. *RBCs classification, filler weight %, filler size, K_{IC}*

	Classification		Filler Weight [%]			Filler Size [nm]			K_{IC} [MPa $m^{0.5}$]		
			Mean	SD		Min	Max	Range	Mean	SD	
Activia Bioactive	RMGI	Bimodal	55.17	0.48	l	91.28	1990	1899	1.48	0.22	b
Admira Fusion	Nanohybrid	Bimodal	84.90	1.43	b	43.82	2669	2625	0.85	0.07	jk
Beautifil II	Hybrid	Bimodal	79.00	0.10	c	164.20	5560	5396	1.14	0.08	fgh
Beautifil Bulk	Hybrid	Bimodal	74.71	0.08	de	50.75	5560	5509	1.07	0.07	gh
Beautifil Bulk Flow	Hybrid	Unimodal	68.40	0.49	i	342.00	3091	2749	1.34	0.10	c
Clearfil Majesty Posterior	Nanohybrid	Bimodal	88.90	0.23	a	32.67	4801	4768	1.29	0.09	cde
Durafill VS	Microfill	Multimodal	57.18	0.16	kl	68.06	1990	1922	0.72	0.03	kl
EPIC TMPT	Microfill	Multimodal	46.59	0.07	m	43.82	1106	1062	0.84	0.09	jk
Filtek One Bulk	Nanohybrid	Bimodal	71.43	0.28	gh	141.80	4801	4659	1.55	0.08	b
Filtek Supreme Ultra	Nanohybrid	Bimodal	72.80	0.21	efg	190.10	5560	5370	1.18	0.08	defgh
GC Kalore	Nanohybrid	Unimodal	69.65	0.14	hi	122.40	3091	2969	1.35	0.14	c
N 'Durance	Nanohybrid	Multimodal	75.00	0.71	d	37.84	3580	3542	0.92	0.06	ij
Point 4	Hybrid	Unimodal	73.84	0.00	def	105.70	1718	1612	1.06	0.13	hi
Renamel Microfill	Microfill	Multimodal	57.53	0.33	k	24.36	2305	2281	0.67	0.07	l
Renamel Nano Plus	Nanohybrid	Bimodal	77.96	0.38	c	50.75	4801	4750	1.10	0.14	fgh
Sonic Fill 2	Hybrid	Bimodal	72.26	0.35	fg	91.28	2669	2578	1.16	0.13	efgh
Tetric Evo Ceram Bulk	Hybrid	Bimodal	73.19	0.20	defg	50.75	3091	3040	1.19	0.12	efg
TPH Spectra ST (HV)	Nanohybrid	Bimodal	73.40	0.05	defg	141.80	4801	4659	1.27	0.09	cdef
Venus Diamond	Nanohybrid	Bimodal	78.17	0.78	c	105.70	3091	2985	1.70	0.12	a
Venus Diamond Flow	Nanohybrid	Bimodal	62.98	1.11	j	141.80	4145	4003	1.31	0.13	cd

Within the column, the same case letter is not significantly different than each other ($p > 0.01$)

RMGI = resin modified glass ionomer; K_{IC} = fracture toughness

Figure 1: Effect of matrix chemistry and filler morphology, system, and distribution on fracture toughness. Asterisk indicates statistically significant differences ($p < 0.01$); columns with same case letters and bracket are not statistically significant ($p > 0.01$).

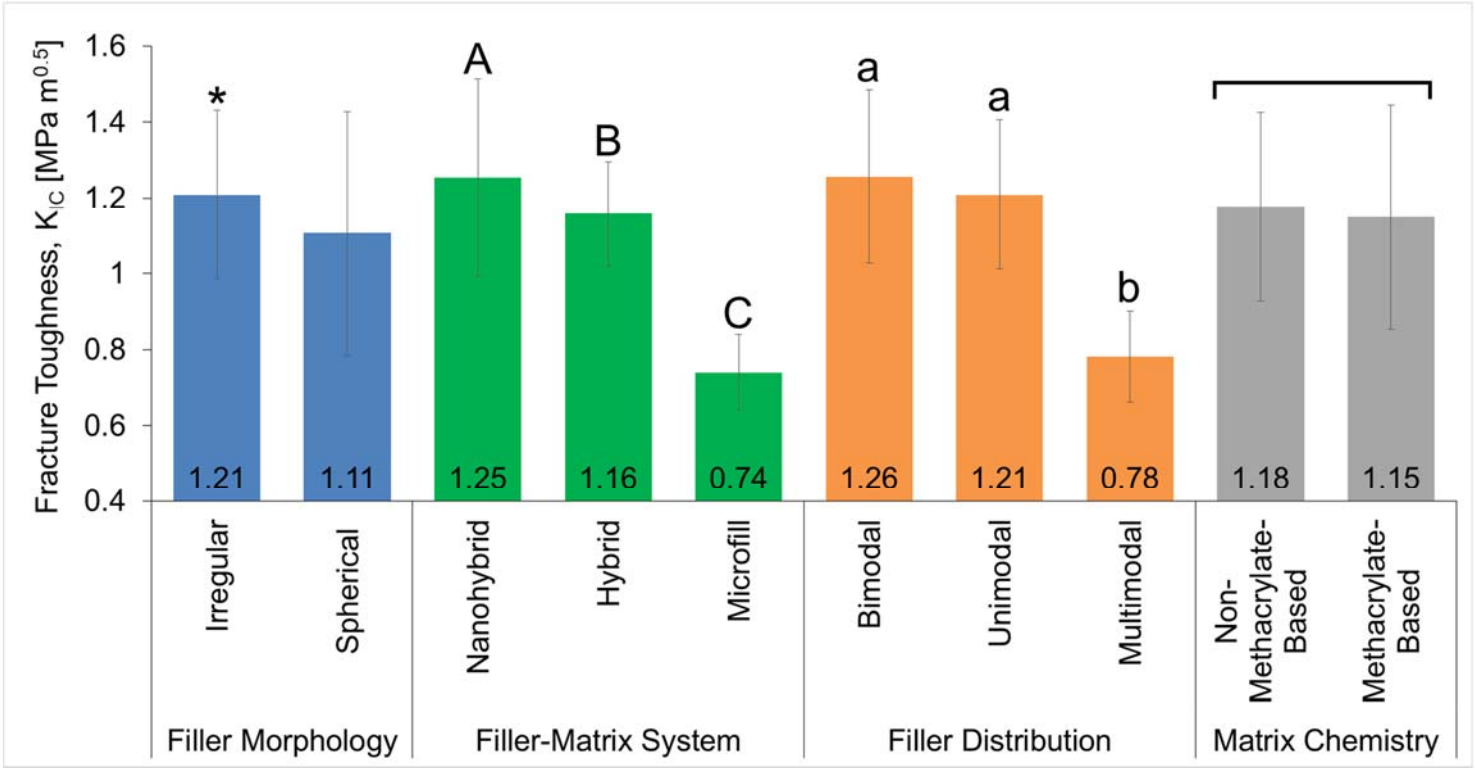

Figure 2: Fracture toughness as a function of filler weight.

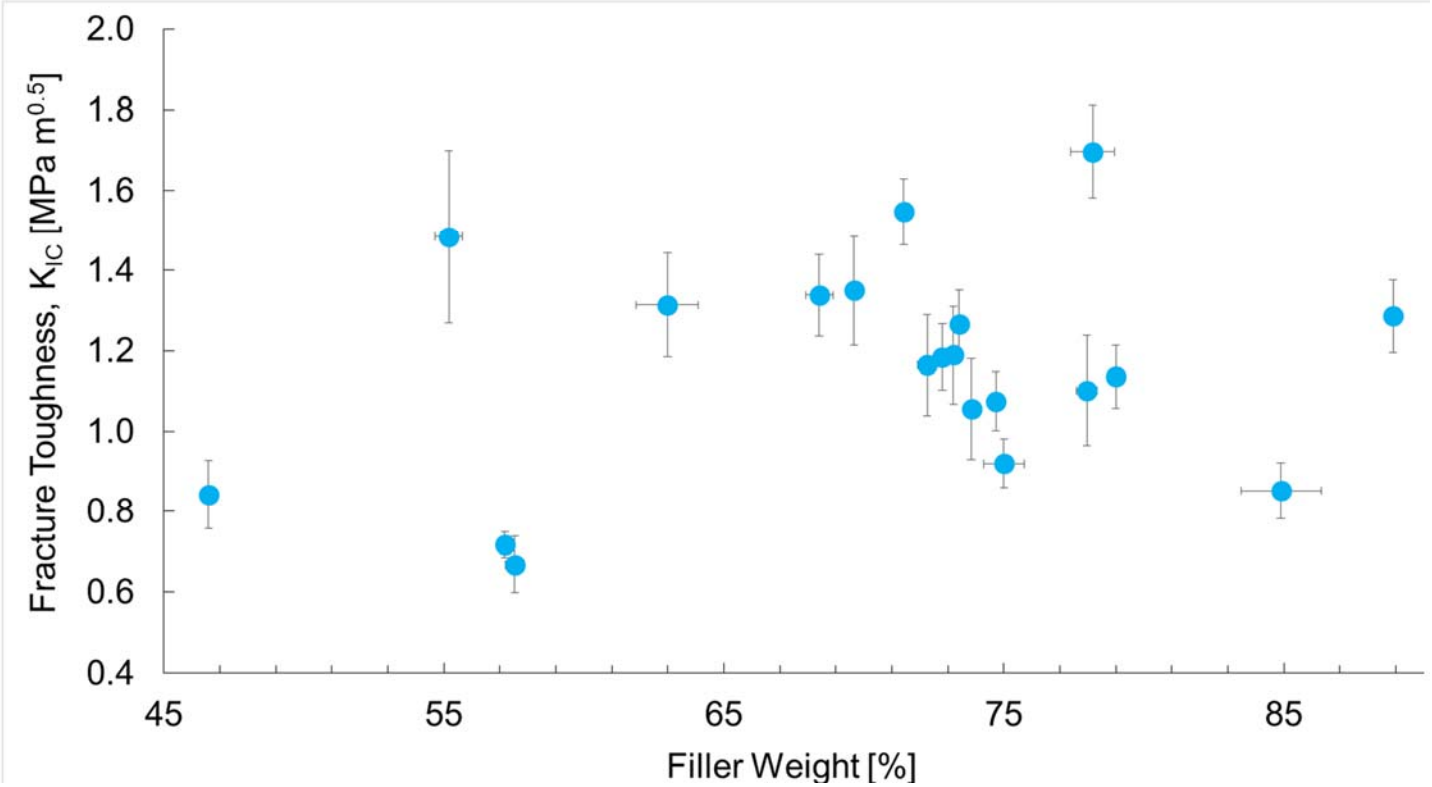

Figure 3: Fracture toughness as a function of filler median size [nm] with special emphasis on mapping clusters of Unimodal, Bimodal, and Multimodal distributions.

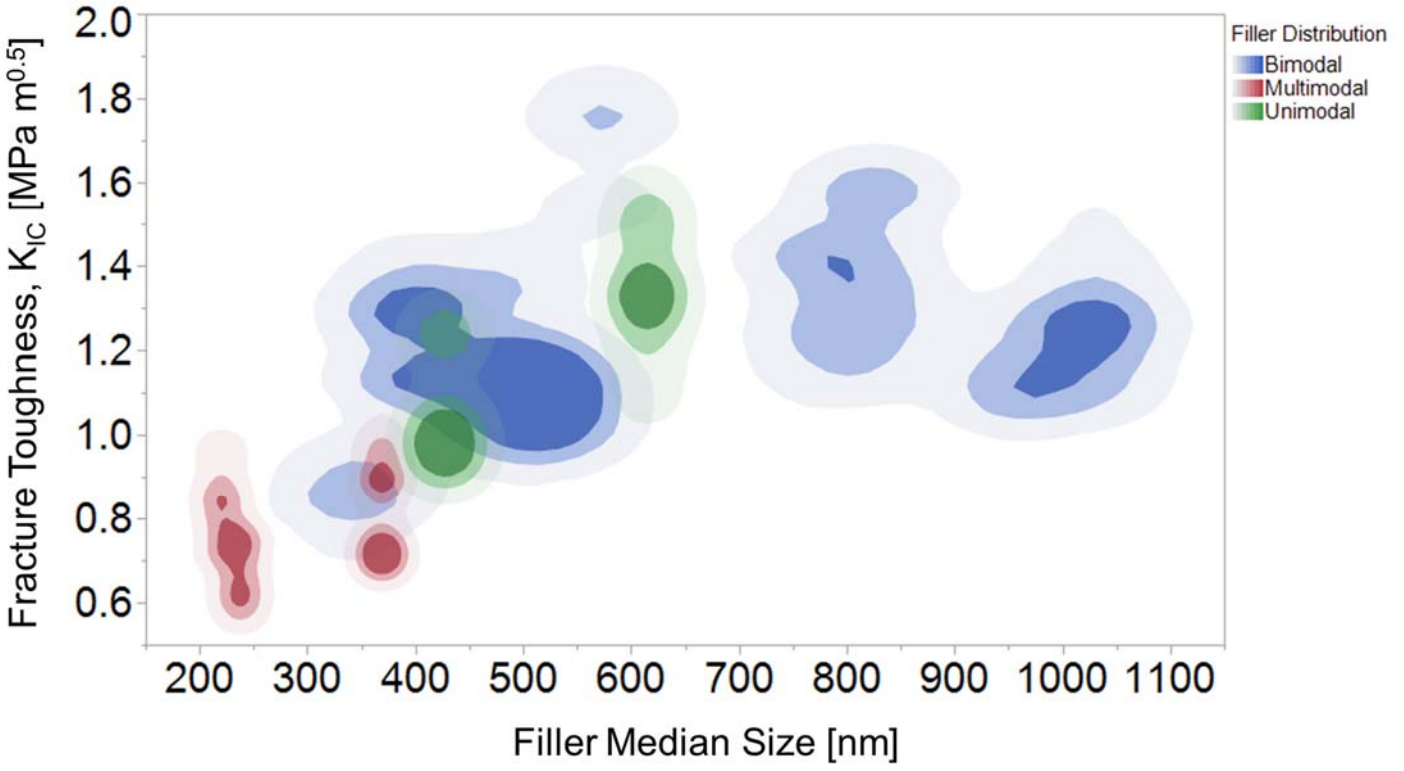

Figure 4a,b,c,d: *Filler sizes, dynamic light scattering method (Zetasizer Nano ZS).*

4a: Admira Fusion (AB), Renamel Nano Plus (RNP), Epic TMPT (ETMPT), Renamel (RM), Admira Fusion (AF), Durafill VS (DVS)
y- axis intensity (%) vs x-axis filler size (nm) distribution

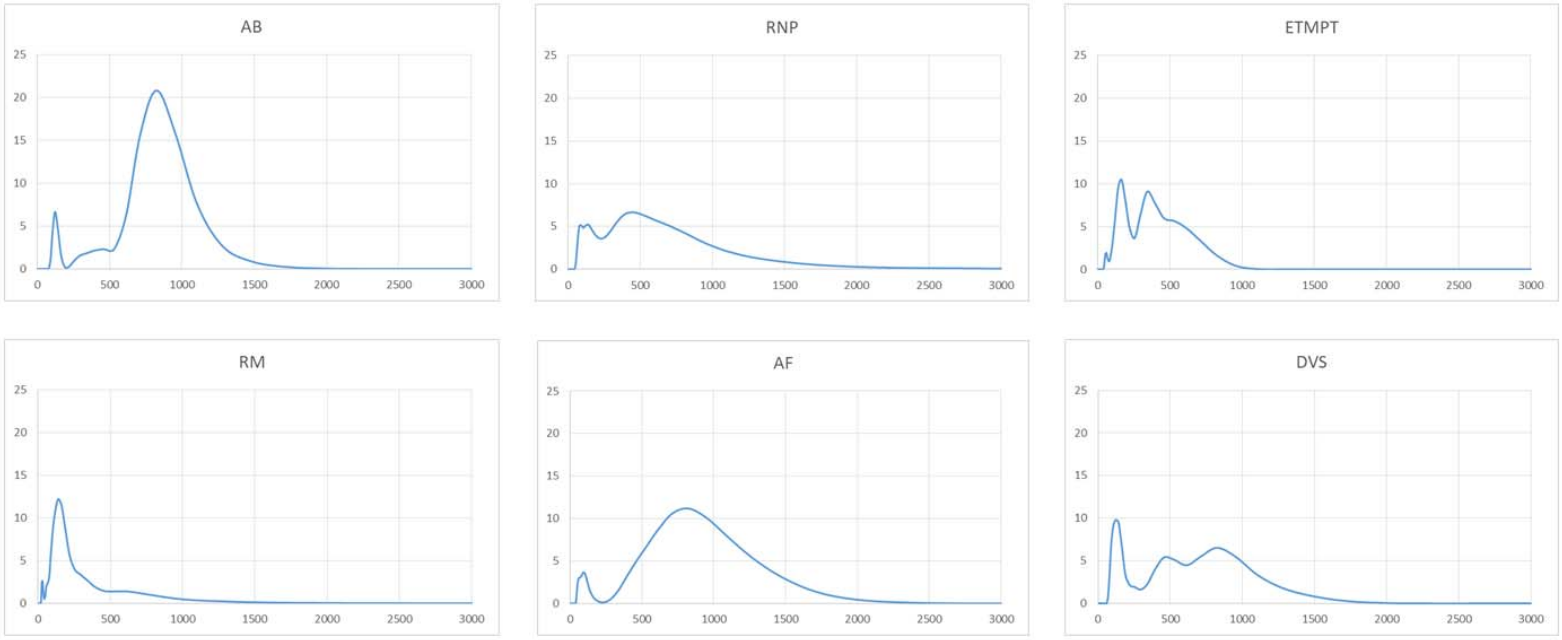

4b: GC Kalore (GCK), N'Durance (ND), Venus Diamond Flow (VDF), Beautifil Bulk Flow (BBF), Point 4 (P4), TPH Spectra HV (TPH-S-HV)
y- axis intensity (%) vs x-axis filler size (nm) distribution

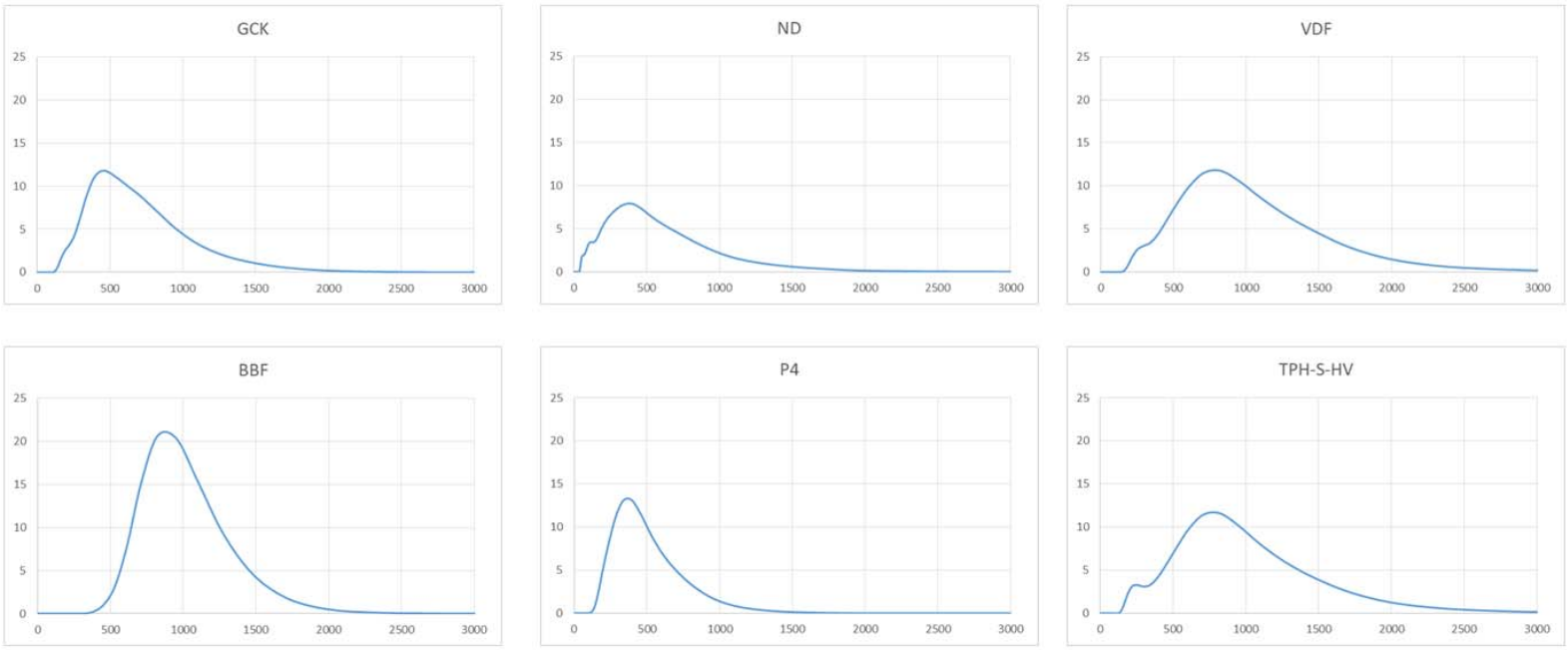

4c: Beuatifil II (BII), Venus Diamond (VD), FIltek Supreme Ultra (FSU), Beautiful Bulk (BB), Clearfill Majesty Posterior (CMP), Tetric Evo Ceram (TEC)
y- axis intensity (%) vs x-axis filler size (nm) distribution

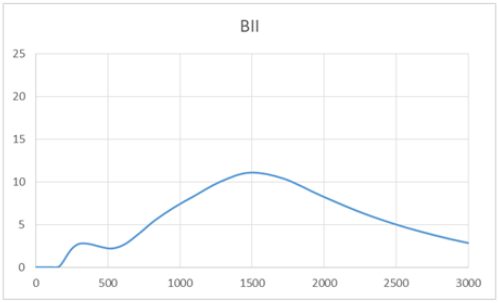

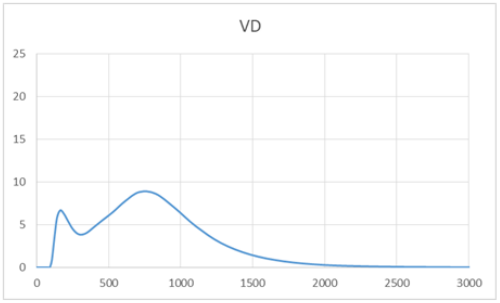

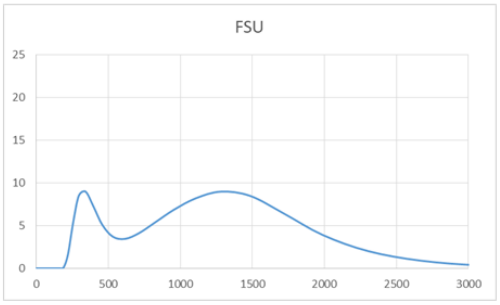

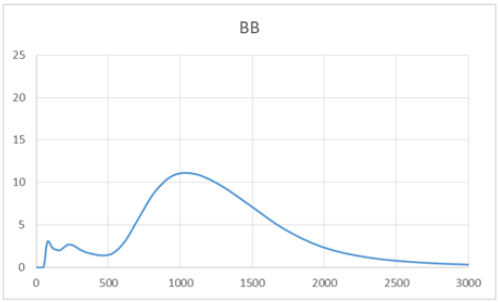

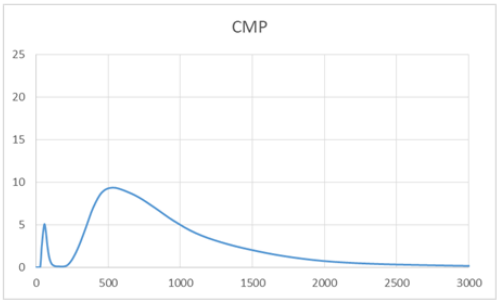

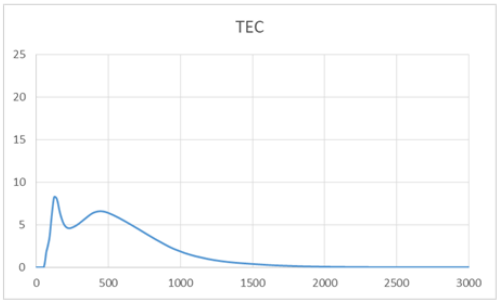

4d: Filtek One Bulk Fill(FOB), Sonic Fill 2 (SF2)
y- axis intensity (%) vs x-axis filler size (nm) distribution

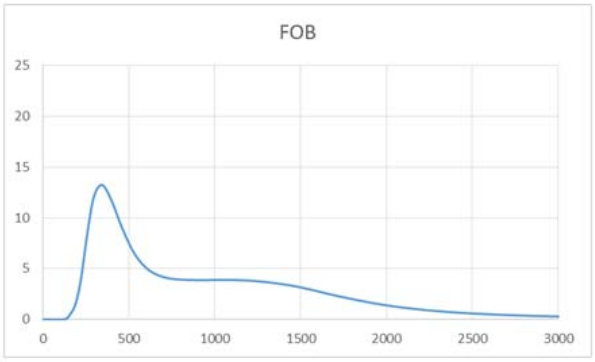

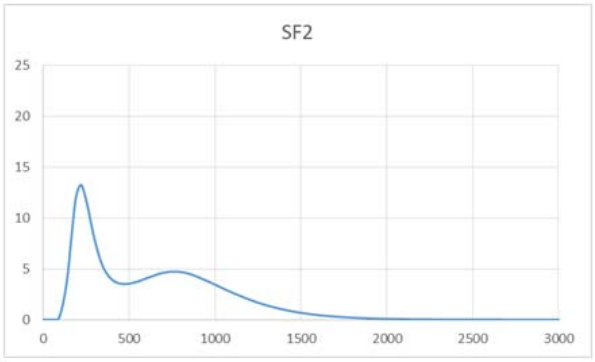

Figure 5a,b,c: *RBCs matrix/filler SEM images*

5a: BB, BII, FOB, FSU, RM, RNP, VD, VDF

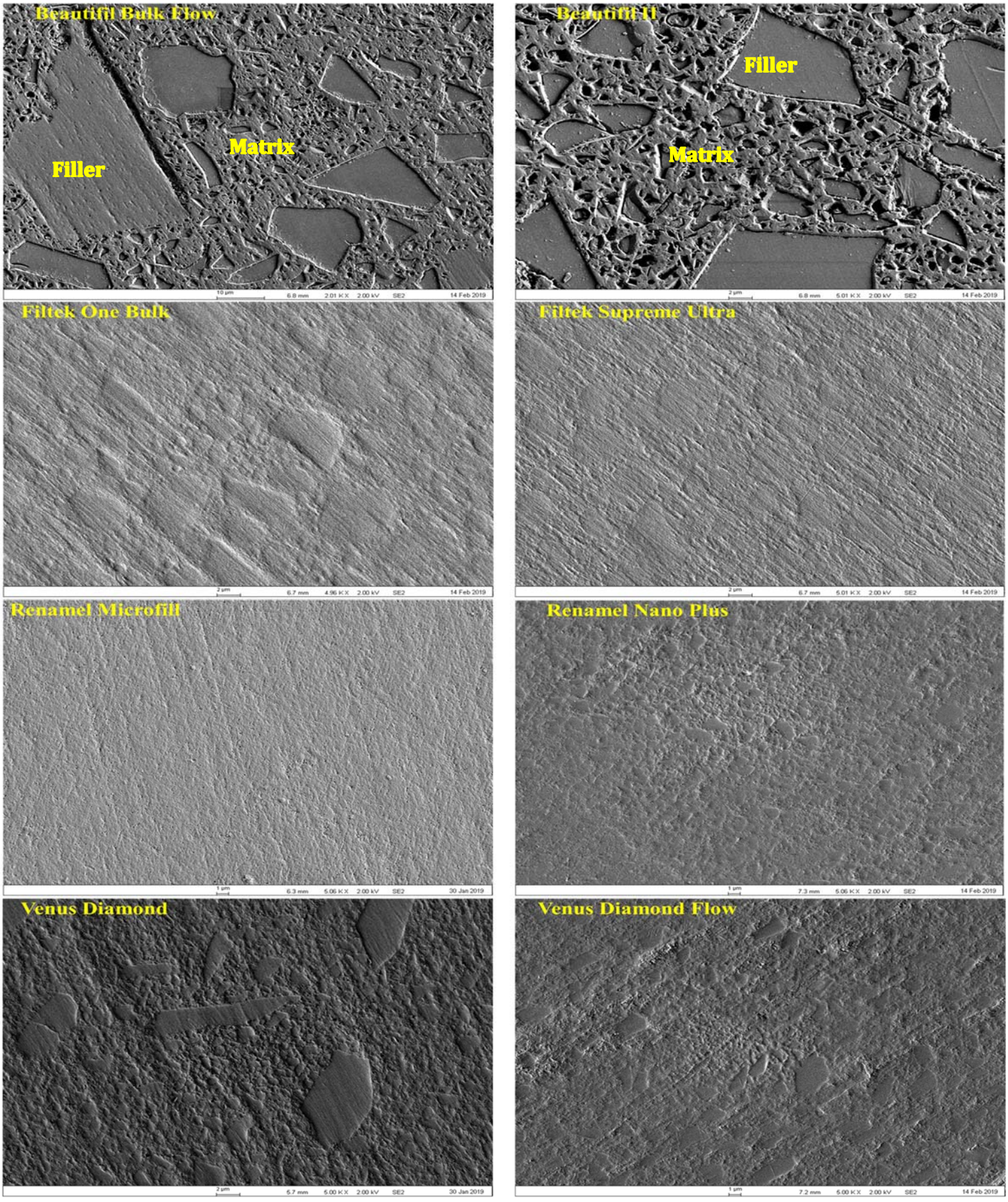

5b: AB, AF, CMP, DVS, GCK, ND, SF2, TECB.

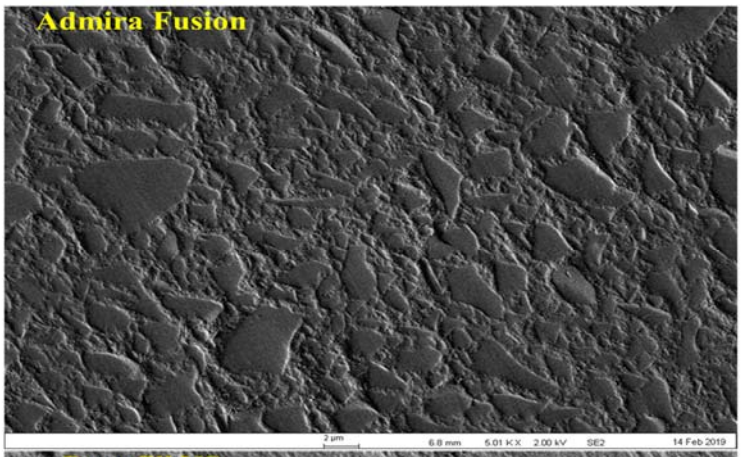

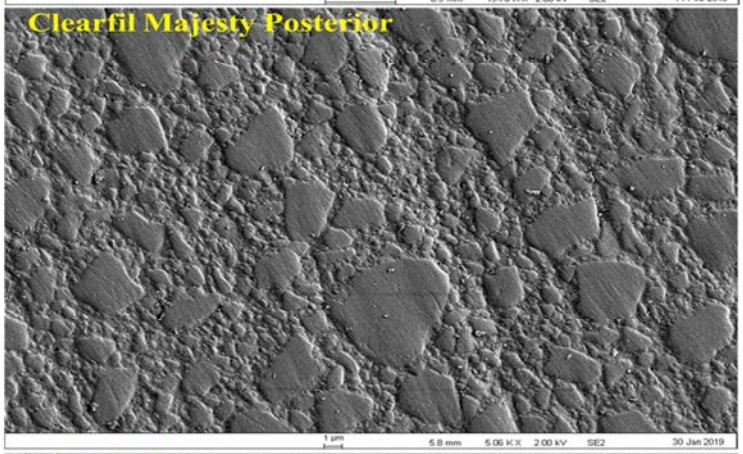

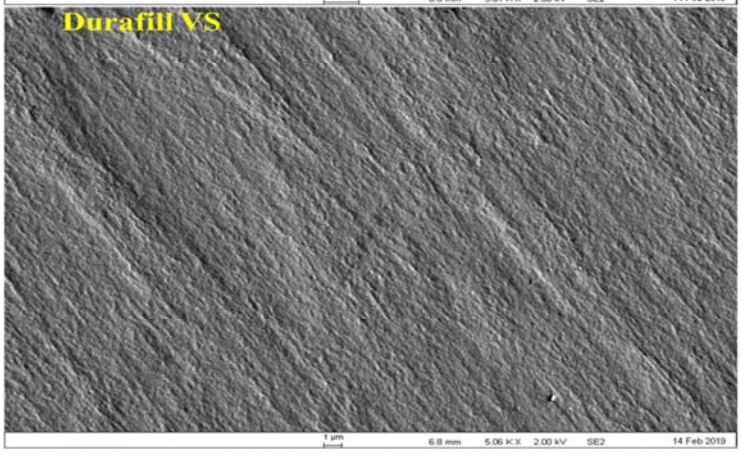

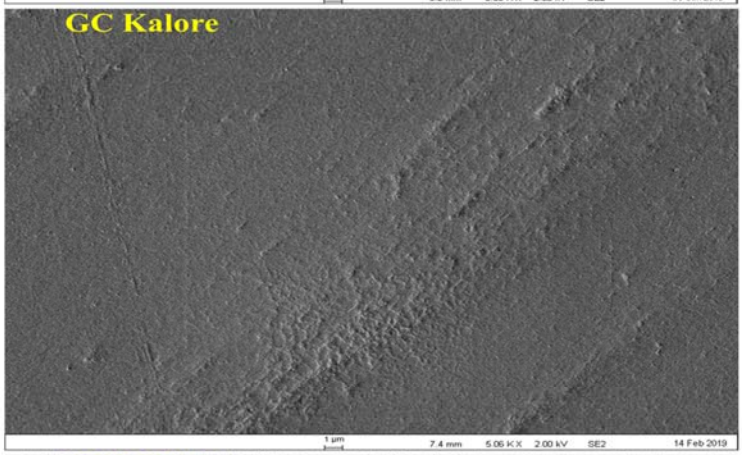

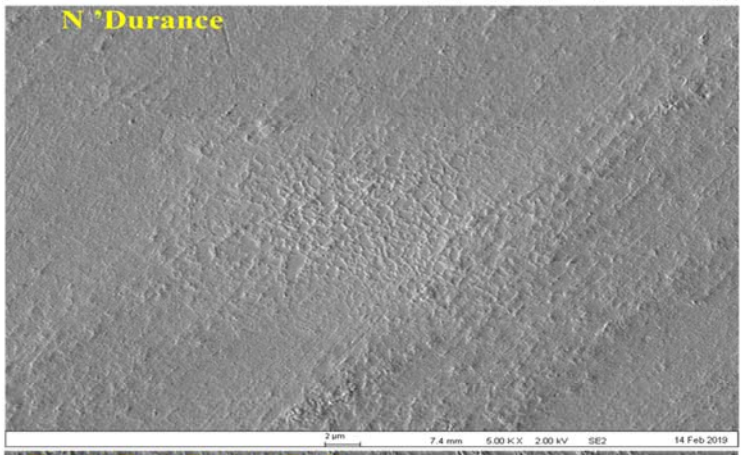

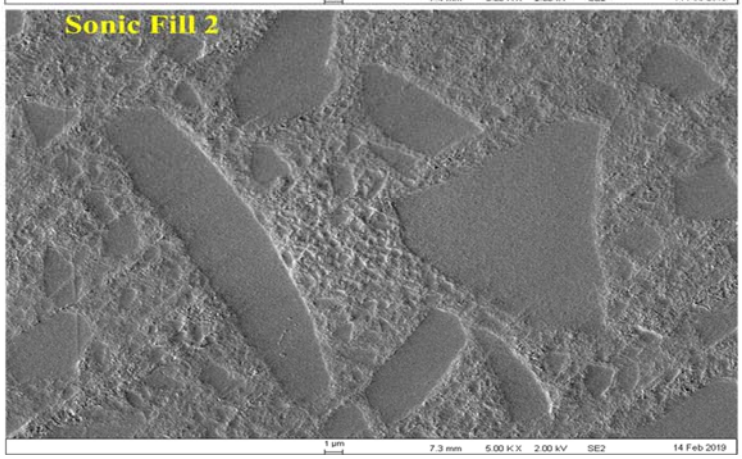

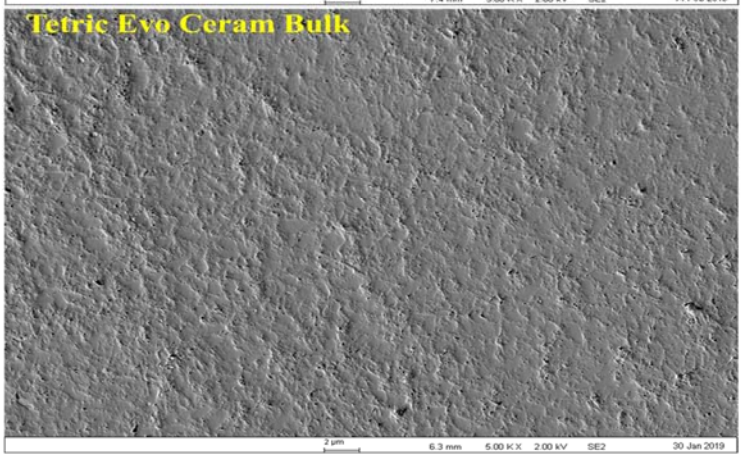

5c: BB, ETMPT, P4, TPH-HV.

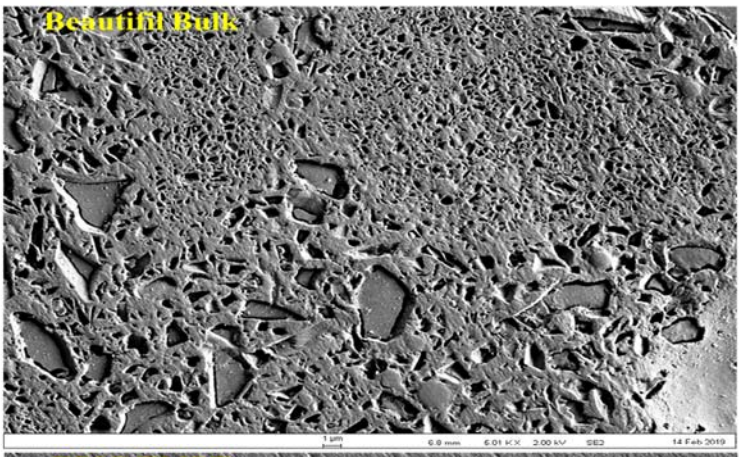

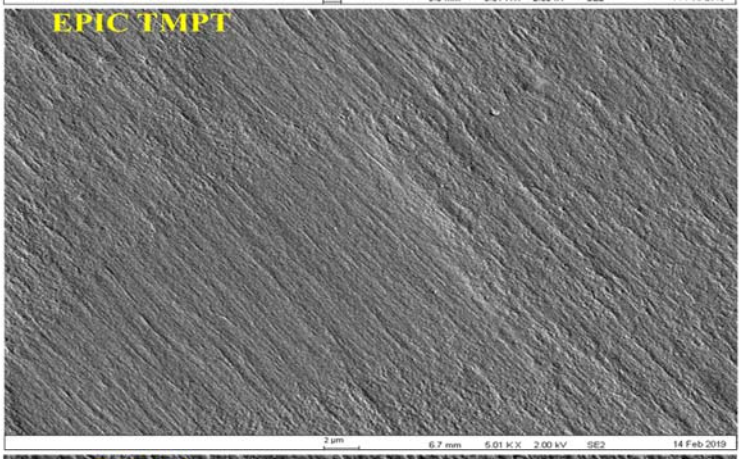

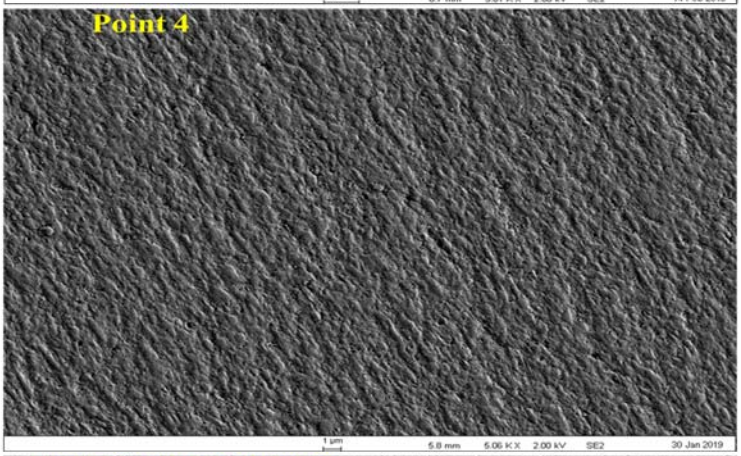

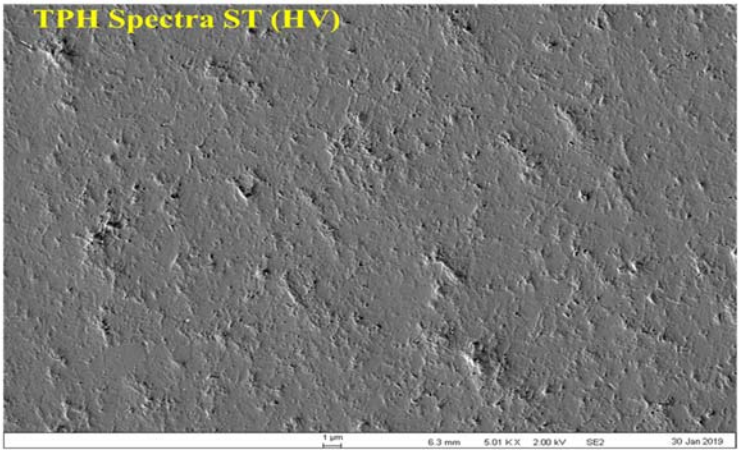

Figure 6 Fracture toughness as a function of filler median size [nm].

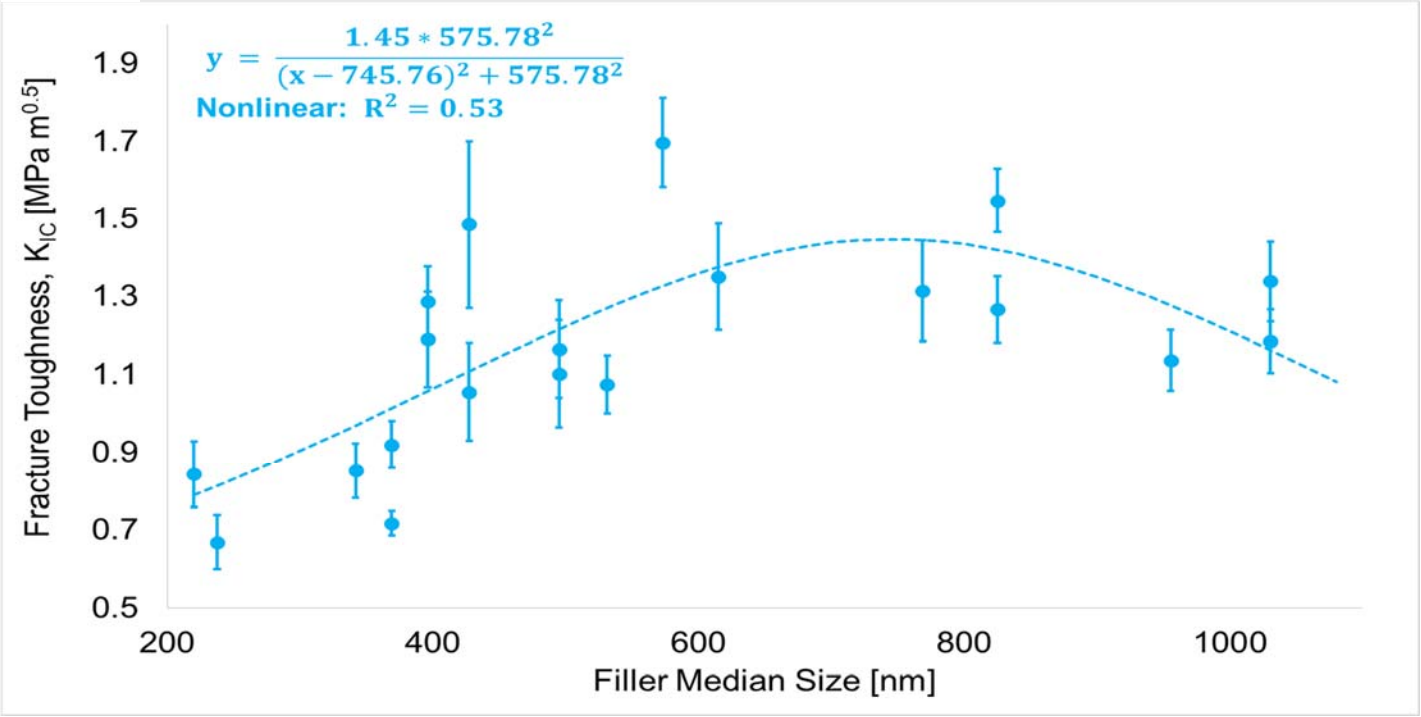

Discussion

In the data collected fracture toughness values showed great variation, ranging from 0.72MPa to 1.70MPa. Fracture toughness was the highest in Nanohybrids and the lowest in Microfills. These results can be presumed to be directly related to the decreased in filler weight %. In their research Ilie, et al, concluded that filler weight % has the strongest influence on the mechanical properties of RBCs.

Ferracane, et al, concluded that fracture toughness was highest in the more heavily filled resins. They stated that there is an increase in the fracture surface area, compared with that of an unfilled resin, due to the presence of the filler particles. Filler particles cause a deflection in the direction of the crack leading it to navigate between particles, thereby increasing the fracture energy and consequently the fracture toughness.

Composites with multimodal distribution demonstrated significantly less fracture resistance than composites with either unimodal or bimodal distribution. From Figure 4(a,b,c,d) it can be deducted that the differences observed in multimodal distributions vs other distributions are due to the decreased size of filler particles (~200-420nm). A possible explanation could be unoccupied areas in the matrix by filler particles. Greater particle size and greater distribution of these particles, allow the filler to occupy a greater zone within the matrix. In the case of multimodal distribution, filler voided areas in the matrix can lead to an increased probability of ease of crack propagation, when compared to unimodal (~350-700nm) and bimodal distributions (~250-1100nm).

Fracture toughness (K_{IC}) as function of the independent variable, filler weight, showed an increased until a critical value of 75%. After filler content of 75% a decreased in fracture toughness as filler weight increased was observed. In a similar fashion, Ilie,

Hickel, Valceanu, Huth observed a straight increased in K_{IC} until a filler weight critical value of 78%, after which the fracture toughness value decreased. A likely cause for the decrease in fracture toughness is the increase in viscosity observed as the filler % increases. This increase in viscosity could increase the introduction of flaws in the resin based composites.

It was observed that the fracture toughness of composite systems adopted with new polymeric matrix chemistry (i.e., ormocer, dimer acid-base, giomer, and DX-511 monomers) were not statistically different than methacrylate-based systems. In our research, the difference of the means between the K_{IC} values of methacrylate-based RBCs and new polymeric matrix chemistry RBCs was 0.03MPa ($p=0.04$), which was not statistically significant.

Irregular filler morphology was correlated with a higher K_{IC} value when compared to spherical morphology. It can be deducted that the irregular morphology can assist with crack deflection, therefore increasing fracture toughness until a critical point is reached were catastrophic failure occurs.

Conclusion

Fracture toughness as a function of filler content increased with percent filler weight until a critical value of 75%, after which K_{IC} decreased with increasing percent filler weight. In a similar behavior, fracture toughness as a function of filler median size exhibited the highest fracture resistance at a critical value of 750nm (Fig 6). However, composites containing nano-fillers showed significantly higher fracture resistance than composites containing only micro-fillers. The fracture toughness of composite systems adopted with new polymeric matrix chemistry (i.e., ormocer, dimer acid-base, giomer, and DX-511 monomers) are not statistically different than methacrylate-based systems.

It can be concluded that filler content is an important factor that should be evaluated when choosing a direct restorative material for its mechanical properties. When choosing a RBC for stress-bearing areas, it is best to use a material with a high filler content since there is a positive correlation between fracture toughness values and percent filler weight. On the other hand, in areas of low stress where there is a greater need for high polish and esthetics, a microfill resin base composite will be best suited.

REFERENCES

1. Farah, J. W., & Powers, J. M. (1991). Anterior and posterior composites. Dent Advisor l99h8: l-8.

2. Ferracane, J. L. (2011). Resin composite—state of the art. Dental materials, 27(1), 29-38.

3. Ferracane, J. L., Antonio, R. C., & Matsumoto, H. (1987). Variables Affecting the Fracture Toughness of Dental Composites. Journal of Dental Research, 66(6), 1140-1145.

4. Ilie, N., Hilton, T., Heintze, S., Hickel, R., Watts, D., Silikas, N., Stansbury, J., Cadenaro, M., & Ferracane, J. (2017). Academy of Dental Materials Guidance: Resin composites: Part I –Mechanical Properties, 33, 880-894.

5. Ilie, N., Hickel, R., Valceanu, A. S., & Huth, K. C. (2012). Fracture toughness of dental restorative materials. Clinical Oral Investigations, 16(2), 489-498.

6. Randolph, L. D., Palin, W. M., Leloup, G., & Leprince, J. G. (2016). Filler characteristics of modern dental resin composites and their influence on physico-mechanical properties. Dental Materials, 32(12), 1586-1599.

7. Nadarajah, V., Neiders, M. E., & Cohen, R. E. (1997). Local inflammatory effects of resin composites. Dent, 18, 367-374.

8. Powers, John M., Ronald Sakaguchi. Craig's Restorative Dental Materials, 12th Edition. C.V. Mosby, 2006.

9. Sakaguchi, R. L., & Powers, J. M. (2012). Restorative materials-composites and polymers. Craig’s Restorative dental materials, 13.

10. Thomaidis, S., Kakaboura, A., Mueller, W. D., & Zinelis, S. (2013). Mechanical properties of contemporary composite resins and their interrelations. Dental materials, 29(8), e132-e141.

11. Tyas, M. J., Alexander, S. B., Beech, D. R., Brockhurst, P. J., & Cook, W. D. (1988). Bonding—retrospect and prospect. Australian dental journal, 33(5), 364-374.